ACS APPLIED MATERIALS & INTERFACES

Research Article

www.acsami.org

Sonochemical Synthesis of Hydrophilic Drug Loaded Multifunctional Bovine Serum Albumin Nanocapsules

Zhanfeng Li,[†] Ting Yang,[†] Chunming Lin,[†] Quanshun Li,[‡] Songfeng Liu,[†] Fengzhi Xu,[†] Hongyan Wang,[†] and Xuejun Cui*[,†]

[†]College of Chemistry and [‡]College of Life Sciences, Jilin University, Changchun 130012, China

Supporting Information

ABSTRACT: A facile sonochemical approach is designed to fabricate protein nanocapsules for hydrophilic drugs (HDs), and HD-loaded multifunctional bovine serum albumin (BSA) nanocapsules (MBNCs) have been prepared for the first time. The as-synthesized HD-loaded MBNCs have a satisfying size range and an excellent magnetic responsive ability. Moreover, high-dose hydrophilic drugs could be loaded into the MBNCs. As carriers, HD-loaded MBNCs also show attractive redox-responsive controlled release ability for hydrophilic drugs and could be internalized selectively by the tumor cells through the folate-mediated endocytosis.

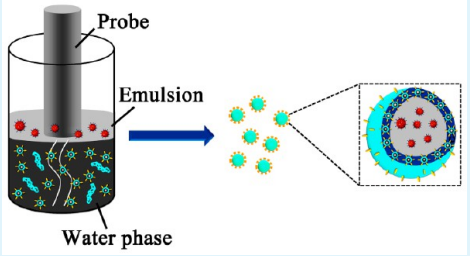

KEYWORDS: *sonochemical, nanocapsule, hydrophilic drug, magnetic responsive, redox-responsive*

1. INTRODUCTION

As a promising delivery system of nanometer or micrometer size ranges, protein nanocapsules and microcapsules have been a focus for many years, especially in the biological field and for the medical needs of biocompatible, biodegradable, and nontoxic materials.[1−4] Certainly, many efforts have been propelled to design and prepare a variety of protein nanocapsules or microcapsules via numerous techniques, such as chemical cross-linking, solvent evaporation method, microemulsion technology, microfluidic fabrication technique, layer-by-layer self-assembling, and so on.[5−8]

In recent years, sonochemistry has been developed rapidly as a novel preparation method, and sonochemical synthesis of protein nanocapsules or microcapsules has drawn our eyes owing to its advantages as follows.[9−11] (i) The sonochemical synthesis is a simple, easy, and short-time physicochemical process dependent on the high-intensity ultrasound.[12] (ii) Through the sonochemical process, high dosage of hydrophobic drugs can be directly loaded into the protein nanocapsules or microcapsules along with the water-insoluble solvent, which avoids destroying their structures.[13−15] (iii) Although the fabrication of the protein nanocapsules and microcapsules is attributed to the sulfydryl cross-linking of the cysteine in the protein molecules, it does not affect the major α-helical structure and properties of protein molecules, for instance, biocompatibility and hydrophilicity, etc.[16] (iv) The cross-linked disulfide bonds are easily broken in a reducing environment, so protein nanocapsules or microcapsules may control the release of hydrophobic drugs.[17−19] (v) There are plenty of residual active groups (carboxyl, amino, etc.) in the as-synthesized protein nanocapsules or microcapsules; thus, various multifunctional protein nanocapsules or microcapsules can be fabricated further by modifying some functional groups or molecules.[20,21] So far, there have been many reports about the sonochemical synthesis of the protein nanocapsules or microcapsules with various properties.[12,20,21]

However, the sonochemical fabrication of the protein nanocapsules or microcapsules often occurs in the oil/water interface or gas/water interface;[9,12] therefore, hydrophobic drugs dispersed in the oil phase can be easily encapsulated into the protein nanocapsules or microcapsules while hydrophilic drugs (HDs) have no access. Hence, the development of the protein nanocapsules or microcapsules is restricted as drug carriers at some level due to their specialized loading for hydrophobic drugs.

Herein, a novel facile sonochemical fabrication of the protein nanocapsules is designed for the HDs for the first time, and HDs are loaded in multifunctional BSA nanocapsules (MBNCs) successfully. In the synthesis, folic acid (FA) and Fe_3O_4 magnetic nanoparticles (Fe_3O_4 MNPs)[22] are immobilized onto the BSA nanocapsules (BNCs) as targeted materials for the special delivery of the drugs, and meanwhile hydrophilic rhodamine B (RhB) is encapsulated into the MBNCs as a model of the HDs. Through the subsequent analysis, the as-synthesized MBNCs show a good magnetic property, FA-mediated selectivity to tumor cells, and inherent redox-responsive ability. Hence, it is confidently believed that MBNCs will be good smart carriers for hydrophilic drugs.

2. EXPERIMENTAL SECTION

2.1. Materials. Ferrous chloride tetrahydrate ($FeCl_2{\cdot}4H_2O$, >99%) and ferric chloride hexahydrate ($FeCl_3{\cdot}6H_2O$, >99%) were purchased from Tianjin Guangfu Chemical Reagents Company (Tianjin, China). Aqueous ammonia (NH_4OH, 25%), *N*,*N*-dimethylformamide (DMF), and sodium citrate ($C_6H_5Na_3O_7$, >99.0%) were purchased from Beijing Chemical Reagent Company (Beijing, China). Span-80 was purchased from Aladdin Industrial Corporation (Shanghai, China). Bovine serum

Received: June 22, 2015
Accepted: August 14, 2015
Published: August 14, 2015

DOI: 10.1021/acsami.5b05558
ACS Appl. Mater. Interfaces 2015, 7, 19390−19397

albumin (BSA), 1-ethyl-3-(3-dimethylaminepropyl) carbodiimide hydrochloride (EDC), and *N*-hydroxysuccinamide (NHS) were purchased from Shanghai Boao Biochemical Technology (Shanghai, China). Folic acid (FA), glutathione (GSH), gelatin, rhodamine B (RhB), and coumarin 6 (C6) were purchased from Sinopharm Chemical Reagent Limited Corporation (Shanghai, China). Phosphate buffers solution (PBS) was prepared by us. Other chemicals were of analytical grade and were used without further purification.

2.2. Synthesis of BSA@Fe_3O_4 MNPs. Fe_3O_4 MNPs with an average particle size of 20 nm were prepared through a chemical coprecipitation process.[23] Then, BSA (100 mg), EDC (100 mg), and NHS (70 mg) were dissolved in the PBS (pH 6.3), and the constant mechanical stirring was carried out for 30 min to activate the carboxyl groups of BSA molecules. At the same time, the as-synthesized Fe_3O_4 MNPs (50 mg) was dispersed into the PBS (pH 6.3) under the ultrasound, forming Fe_3O_4 magnetic fluid. Afterward, Fe_3O_4 magnetic fluid was added to the BSA solution to be coated with BSA molecules. After fast stirring for 24 h in the 20 °C water bath, the core−shell BSA@Fe_3O_4 MNPs were collected and washed to remove the unreacted BSA molecules. Finally, BSA@Fe_3O_4 MNPs were dispersed into the deionized water.

2.3. FA Conjugated BSA@Fe_3O_4 MNPs. FA (5 mg), NHS (42 mg), and EDC (60 mg) were dissolved in DMF/PBS solution (v/v = 1:1, pH 6.3) by the stirring. Then, the solution with BSA@Fe_3O_4 MNPs (10 mg/mL) was added into the above-mentioned solution. After the reaction was carried out at room temperature for 24 h, FA functional BSA@Fe_3O_4 MNPs (FA-BSA@Fe_3O_4 MNPs) were collected using an external magnet. FA-BSA@Fe_3O_4 MNPs were dispersed in deionized water at last after being washed several times.

2.4. Preparation of HD-Loaded MBNCs. As a model HD, RhB was dissolved into gelatin solution (60 mg/mL) to make RhB-loaded hydrogel (1.0 mg/mL). Through the high-intensity ultrasound, RhB-loaded hydrogel (1.0 mL) was dispersed into the vegetable oil (10 mL) with surfactant span-80 (0.5 mL) to form an RhB-loaded water/oil emulsion. The RhB-loaded water/oil emulsion (1 mL) was layered on top of the mixed solution (5 mL) containing FA-BSA@Fe_3O_4 MNPs (50 mg/mL) and BSA (1 mg/mL). The emulsion/water mixed solution was laid in the ice bath to maintain the temperature below 20 °C during the ultrasound treatment. Then the probe of an ultrasonicator was inserted into the emulsion/water mixed solution with its tip placed at the emulsion/water interface. An acoustic frequency at 20 kHz was carried out at a 400 W cm^{-2} power for 5 min in the pulse sonication mode (2s/2s). After the sonication, the layered emulsion/water mixed solution turned into a brown suspension. The suspension was cooled naturally, and the resultant RhB-loaded MBNCs were separated from the suspension under the outer magnetic field and then washed several times and redispersed in deionized water (100 mg/mL).

2.5. Controlled Release of RhB-Loaded MBNCs. The as-synthesized RhB-loaded MBNCs suspension (4 mL) was injected into dialysis tubing (8000). The dialysis tubing was immersed completely into the vessel with the PBS dialysate (pH 7.4, 100 mL) containing GSH (10 mM), and then the vessel was vibrated by 100 rpm in the water bath (37 °C). The absorbances of the dialysate at different time were measured by a UV−vis spectrophotometer at the characteristic absorption wavelength (λ = 552 nm), and the measurements were recorded. The absorbance of RhB in the dialysate was a direct diagnostic signal of the released amount of RhB-loaded MBNCs.

2.6. Cellular Uptake and Flow Cytometric Assay. For the cellular uptake of RhB-loaded MBNCs, tumor cells (A549 cells and HeLa cells) were seeded in 12-well plates where there were 1.0×10^5 cells per well and were incubated in serum-free medium for 24 h before the cellular endocytosis. Then the cells in some wells were incubated in serum-free medium with RhB-loaded MBNCs (2.0 mL) while the cells in other wells were still incubated in serum-free medium, and the cells in rest wells were pretreated with FA (10 mg/mL) for 1 h and then incubated in serum-free medium with RhB-loaded MBNCs (2 mL). After all the cells were incubated for another 6 h, they were harvested and washed with PBS (pH 7.4) and then fixed with ethanol (75%). Finally, the morphology of these fixed cells was characterized through the confocal laser scanning microscopy (CLSM).

For the flow cytometric assay, HeLa cells were seeded in 12-well plates where there were 2.0×10^5 cells per well and incubated in serum-free medium for some time. When the cells reached 70%−80% confluence, the cells in some wells were incubated in serum-free medium with RhB-loaded MBNCs (2.0 mL) for 6 h. In the meantime, the cells in other wells after the pretreatment with FA (1 h) were incubated in serum-free medium for 6 h. Subsequently, all the cells were harvested and suspended with PBS (pH 7.4), and then the flow cytometry was carried out using a FACS Calibur instrument.

2.7. Measurements. Transmission electron microscopy (TEM) images were recorded using the JEOL JEM-2100F transmission microscope at an accelerating voltage of 200 kV. The preparation samples dispersed in water were dropped onto an amorphous carbon-coated copper grid and allowed to air-dry at room temperature. The morphology of samples was investigated using the field emission scanning electron microscope (FESEM) with a Hitachi S-4800 FESEM. Confocal laser scanning microscopy (CLSM) images were taken with a confocal laser-scanning system TCLS attached to an inverse microscope (FV1000) from Olympus (Japan). The UV−vis absorption was observed by the UV-2550 spectrophotometer from Shimadzu (Japan). The size distribution of nanoparticles was measured by dynamic light scattering (DLS) with a 90Plus/BI-MAS. Fourier transform infrared spectra (FTIR) of KBr powder-pressed pellets were recorded in the range 400−4000 cm^{-1} on a Nicolet Instruments Research Series 5PC Fourier transform infrared spectrometer. The flow cytometry was evaluated using a FACS Calibur instrument (BD Bioscience Mountain View). The microphotograph was obtained by an optical microscope. Thermogravimetric analysis (TG) was performed with a Pyris 1TGA (PerkinElmer) at a heating rate of 10 °C/min in the nitrogen atmosphere over the range 100−900 °C.

3. RESULTS AND DISCUSSION

3.1. Fabrication of HD-Loaded MBNCs. According to the experiments, synthesis of HD-loaded MBNCs was a multistep process based on the sonochemical method (Scheme 1). First, the core−shell BSA@Fe_3O_4 MNPs were prepared by chemical

Scheme 1. Synthesis Mechanism of (A) FA-BSA@Fe_3O_4 MNPs, (B) HD-Loaded Micelles, and (C) HD-Loaded MBNCs

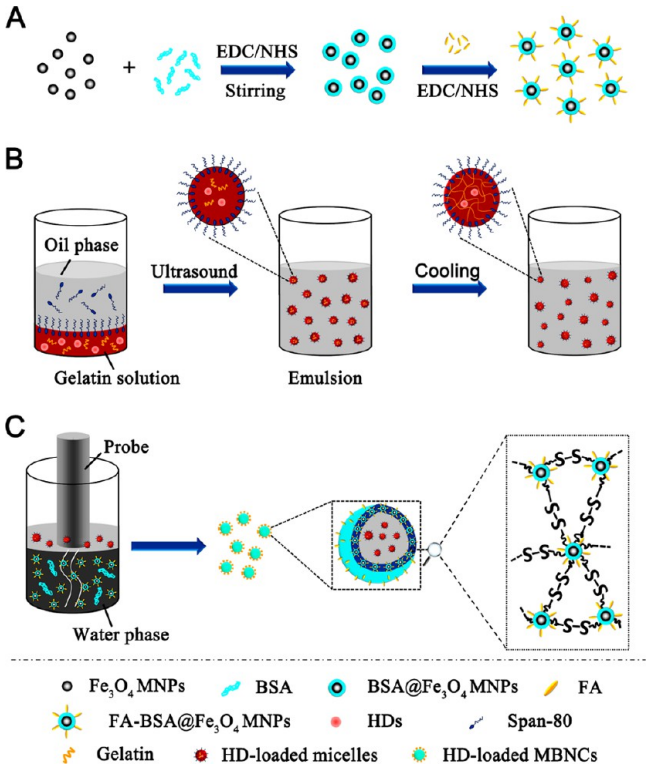

DOI: 10.1021/acsami.5b05558
ACS Appl. Mater. Interfaces 2015, 7, 19390−19397

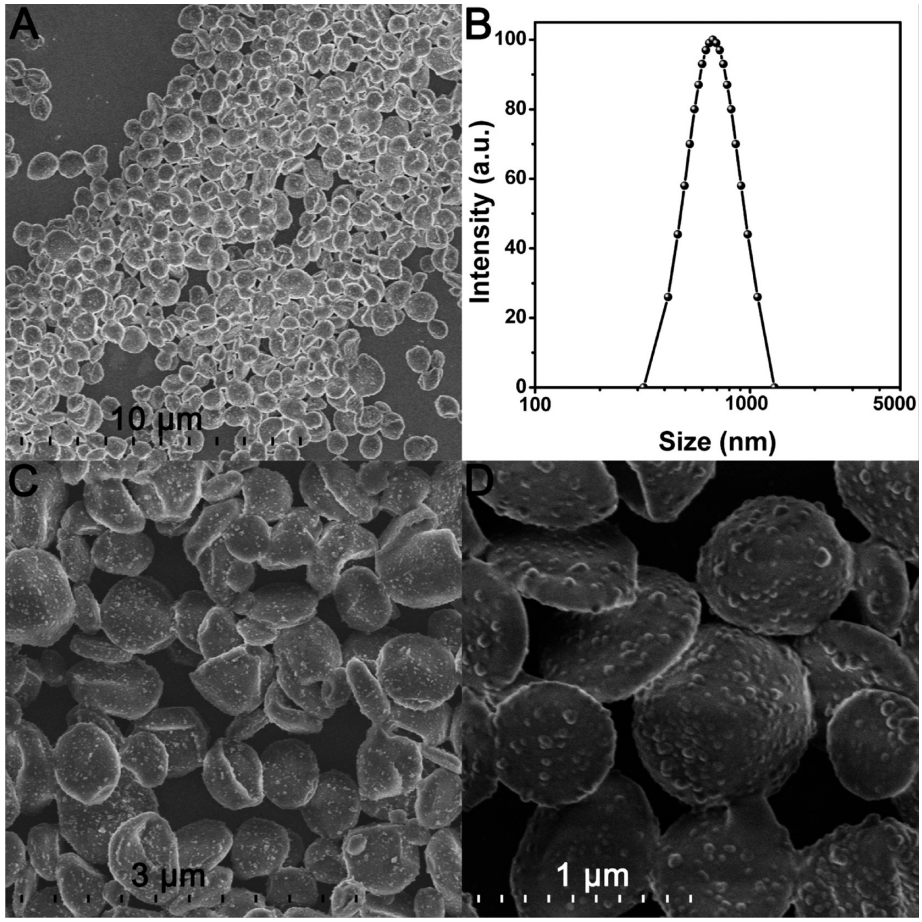

Figure 1. (A, C, and D) SEM images of HD-loaded MBNCs. (B) Size distribution of HD-loaded MBNCs.

bonding, and there were many sulfydryl groups remaining on the surface of the BSA@Fe_3O_4 nanoparticles.[24,25] Then, BSA@Fe_3O_4 nanoparticles were modified with the targeting molecule FA, which was confirmed by FTIR and UV−vis spectra (Figure S1 and Figure S2). Second, HDs were dissolved in the gelatin hydrogel which was thermoresponsive (Figure S3), and then HD-loaded hydrogel liquid was dispersed into the vegetable oil with span-80, forming a water/oil emulsion with a mean size of 57 nm (Figure S4). Afterward, the emulsion cooled down to turn the inner hydrogel liquid into solid phase. Third, HD-loaded emulsion was layered on the top of the mixed solution containing BSA and FA-BSA@Fe_3O_4 MNPs, and then a high-intensity ultrasound was carried out at the emulsion/water interface to fabricate HD-loaded MBNCs, in which BSA molecules and FA-BSA@Fe_3O_4 MNPs were cross-linked to form the shells of the nanocapsules with HD-loaded emulsion being coated as the cores.

3.2. Morphology of HD-Loaded MBNCs. As-synthesized HD-loaded MBNCs were dispersed well in the water, which was ascribed to hydrophilic BSA molecules of the capsule shells. Through the optical microscope, HD-loaded MBNCs in the water showed spherical morphology (Figure S5). SEM images could give us the superfine morphology of HD-loaded MBNCs. As shown in Figure 1A, HD-loaded MBNCs were irregular spheres with size less than 1 μm. The average diameter of HD-loaded MBNCs was about 700 nm by the DLS with a 90Plus/BI-MAS device (Figure 1B), and the size was enough to load the water/oil emulsion and to be relatively practicable for the pharmacological delivery in the bloodstream.[26,27] Enlarging the SEM images, we found most of the HD-loaded MBNCs were collapsed or folded due to the elimination of inner emulsion (Figure 1C), and it proved that HD-loaded MBNCs were soft material actually. When HD-loaded MBNCs were magnified further, the lumpy surfaces of HD-loaded MBNCs were observed clearly on account of the existence of Fe_3O_4 MNPs (Figure 1D).

The microscopic structure of HD-loaded MBNCs was measured by TEM as well. In Figure 2A, HD-loaded MBNCs with irregular morphology were thickly dotted with particle clusters on the capsule walls. These particle clusters were found to be Fe_3O_4 MNPs after adjusting high magnification (Figure 2B). The case was in accord with the results of SEM. Furthermore, through the thermogravimetric analysis (TG), the weight proportion of Fe_3O_4 MNPs was about 12.85% (Figure S6). Because of strong superparamagnetism of Fe_3O_4 MNPs,[28−31] HD-loaded MBNCs promised excellent magnetic responsive properties.

3.3. Magnetic Property of HD-Loaded MBNCs. HD-loaded MBNCs were demonstrated to have magnetic response by the collection and motion of HD-loaded MBNCs in an external magnetic field (Figure 3). When a magnet was placed on one side of the vial containing the brown HD-loaded MBNCs, HD-loaded MBNCs occurred to gather onto the side of the vial close to the magnet in a very short time, forming the aggregation (Figure 3A). After the removal of the magnet, it was easy to redisperse HD-loaded MBNCs into the solution by gentle shaking. While the magnet was close to one side of the vial once more, HD-loaded MBNCs were aggregated again, demonstrating that HD-loaded MBNCs possessed satisfactory magnetic response. Moreover, HD-loaded MBNCs could be manipulated

DOI: 10.1021/acsami.5b05558
ACS Appl. Mater. Interfaces 2015, 7, 19390−19397

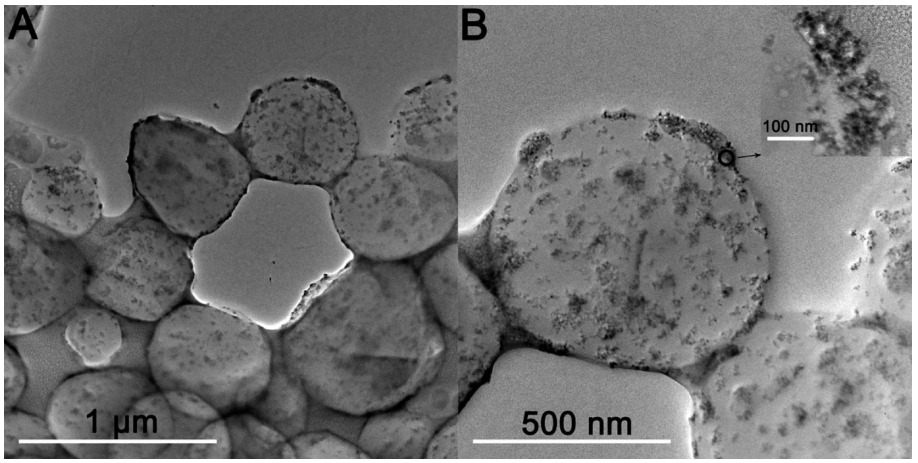

Figure 2. TEM images of HD-loaded MBNCs (A and B).

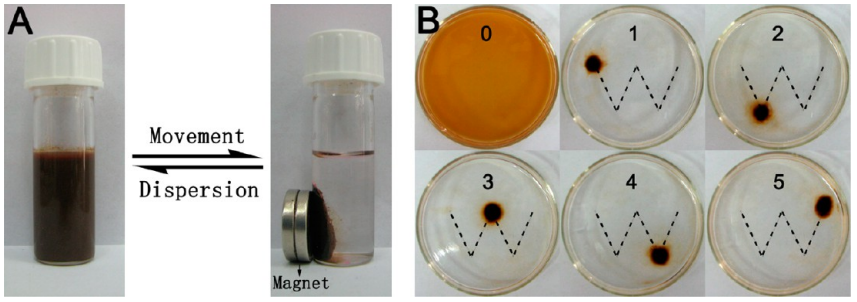

Figure 3. (A) Collection and (B) motion of HD-loaded MBNCs.

to move in a desired direction by an external magnetic field; the location of HD-loaded MBNCs depended on the magnetic field (Figure 3B), and there was little magnetic loss with time. The phenomenon illustrated that HD-loaded MBNCs possessed a good magnetic targeted response which might increase the local drug concentration and improve the therapeutic efficiency.[32,33]

The magnetic property of HD-loaded MBNCs was also confirmed by the VSM measurement. The magnetization curve of HD-loaded MBNCs in Figure 4 showed no detectable coercivity in the field sweep, implying that HD-loaded MBNCs were superparamagnetic. Hence, it could be concluded that the obtained HD-loaded MBNCs had excellent magnetic properties and had access to the field of targeted delivery.

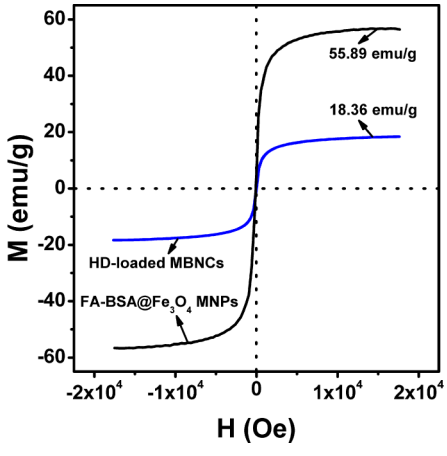

Figure 4. Magnetization curves of FA-BSA@Fe_3O_4 MNPs and HD-loaded MBNCs.

3.4. Loading Capacity of HD-Loaded MBNCs. To confirm whether HDs were encapsulated into the MBNCs, rhodamine B (RhB), a widely used hydrophilic fluorescent dye,[34,35] was loaded into MBNCs as a model HD. CLSM measurement was used to determine the RhB-loaded MBNCs, and the results were showed in Figure 5. The red signals could be seen clearly in the fluorescence mode (Figure 5B) while there were no signals disappearing in the transmission mode (Figure 5A). Obviously, the red fluorescent signals were originating from RhB motivated by the laser. Superimposing the two modes (Figure 5C), we found that the red signals were from the RhB-loaded MBNCs. It demonstrated that the hydrophilic RhB was encapsulated successfully into the MBNCs.

In order to verify the loading mechanism of RhB further, hydrophobic fluorescent dye coumarin 6 was dispersed into the water/oil emulsion and then loaded into the MBNCs. Images D−G in Figure 5 showed the CLSM images of the MBNCs with coumarin 6 and RhB, and both green signals of coumarin 6 and red signals of RhB were from the capsules, which proved clearly that RhB was loaded into the MBNCs along with the water/oil emulsion. Meanwhile, the HD-loaded capacity of the MBNCs was measured by a UV−vis spectrophotometer (Figure 6). Through the absorbance−concentration curve of RhB (Figure S7), we could calculate that there was up to 86.67% of RhB encapsulated into the MBNCs. Accordingly, the MBNCs could be good carriers for the hydrophilic drugs, for example, hydroxyurea (HU), nimustine hydrochloride (ACNU), and cytosine arabinoside (Ara-C), etc.

3.5. Controlled Release. Since HD-loaded MBNCs were closely related to the formation of the disulfide linkage,[36] HD-loaded MBNCs would be disassembled and release inner hydrophilic drugs in the reductive condition (Figure 7A), such as

DOI: 10.1021/acsami.5b05558
ACS Appl. Mater. Interfaces 2015, 7, 19390−19397

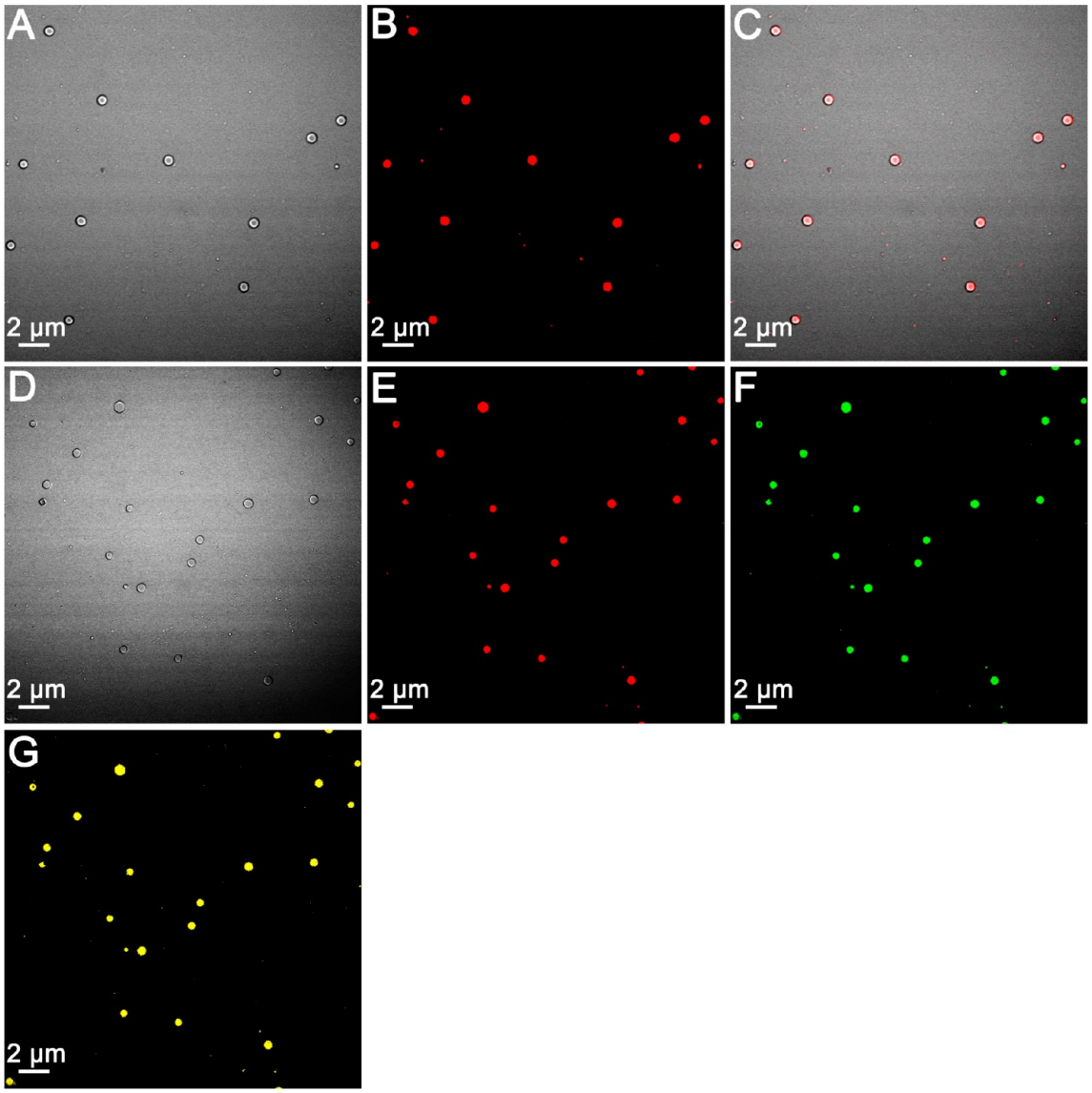

Figure 5. CLSM images of RhB-loaded MBNCs: (A) transmission mode, (B) fluorescence mode, and (C) merged mode. CLSM images of the MBNCs with coumarin 6 and RhB: (D) transmission mode, (E) red fluorescence mode, (F) green fluorescence mode, and (G) merged mode of the red and green fluorescence.

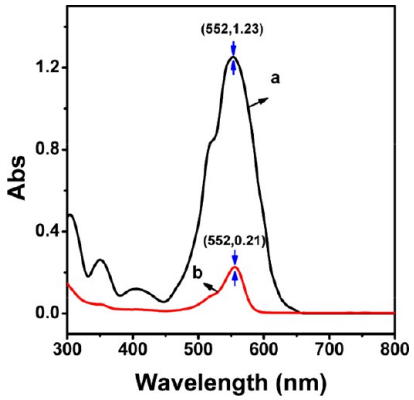

Figure 6. (a) UV−vis spectrum curve of RhB solution (100 μg/mL). (b) UV−vis spectrum curve of RhB released from the MBNCs (1 mL).

DL-dithiothreitol (DTT) and glutathione (GSH);[37−39] that is, HD-loaded MBNCs possessed a redox-sensitive property for drug controlled release. To confirm the controlled release ability of HD-loaded MBNCs, some GSH-triggered disassembly experiments were carried out for the RhB-loaded MBNCs. The RhB-loaded MBNCs were treated in GSH dialysate (10 mM); meanwhile, the release amount of RhB in the dialysate was recorded by the UV−vis spectrophotometer at the maximum absorption wavelength of RhB (λ_{max} = 552 nm),[34,40] and then the time-dependent release curve of the RhB was plotted (Figure 7B). The RhB-loaded water/oil emulsion almost released all the RhB easily. When RhB-loaded water/oil emulsion was encapsulated into the MBNCs by the sonochemical method, the release rate of the RhB-loaded MBNCs decreased sharply, and the final release amount also dropped a lot. By contrast, the release process of the RhB-loaded MBNCs was accelerated obviously in the presence of GSH, and the final release amount was up to 91.42%. These results suggested that HD-loaded MBNCs had excellent controlled release ability for their redox-responsive ability.

3.6. Cellular Selectivity. RhB-loaded MBNCs had many FA molecules on the capsule walls, so we chose A549 cells (lung cancer cells) and HeLa cells (ovarian carcinomas cells) to

DOI: 10.1021/acsami.5b05558
ACS Appl. Mater. Interfaces 2015, 7, 19390−19397

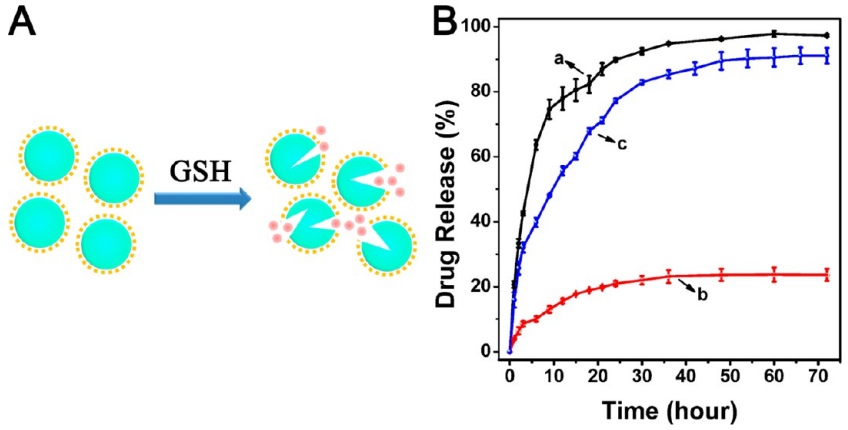

Figure 7. (A) Schematic of the GSH-triggered disassembly of HD-loaded MBNCs; (B) time-dependent release curves: (a) RhB-loaded water/oil emulsion, (b) RhB-loaded MBNCs, and (c) RhB-loaded MBNCs in the presence of GSH.

monitor the cellular internalizing behaviors of HDs-loaded MBNCs.[41,42] CLSM images of tumor cells incubated in the serum-free medium with RhB-loaded MBNCs had been shown in Figure 8. In contrast to A549 cells with fewer folate receptors (FRs) (images A and B), FR-overexpressed HeLa cells had much stronger red fluorescence in the intracellular regions (images C and D);[43,44] however, after the pretreatment of FA, the fluorescent intensity of HeLa cells was weakened a lot (images E and F). These results implied that RhB-loaded MBNCs could be internalized easily by the FR-overexpressed tumor cells.

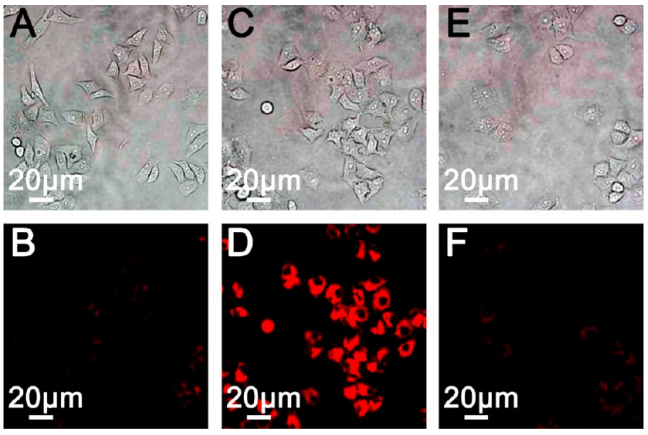

Figure 8. CLSM images of tumor cells incubated in the serum-free medium with RhB-loaded MBNCs: A549 cells (A and B), HeLa cells (C and D), and HeLa cells after the pretreatment of FA (E and F). Among these images, images a, c, and e were in the bright field while images b, d, and f were in the dark field.

The flow cytometry also gave us some insight into the mechanism for cellular internalization of RhB-loaded MBNCs. As Figure 9A showed, the intracellular fluorescent intensity of HeLa cells incubated in pure serum-free medium was very low (curve a). However, the fluorescent intensity of HeLa cells incubated in serum-free medium with RhB-loaded MBNCs was very high (curve c). After HeLa cells were pretreated with FA, the fluorescent intensity was degraded obviously (curve d). The results of the flow cytometric assay were consistent with those in the CLSM images in Figure 8. Thus, we confirmed adequately that RhB-loaded MBNCs could be taken in mainly via the FA-dependent endocytosis (Figure 9B).[45] Certainly, hydrophobic drugs could be loaded into the MBNCs with HDs and internalized by the tumor cells (Figure S8), perhaps improving the pharmacological effects synergistically.

In fact, compared with normal cells, there were abundant GSH species in the tumor cells.[46,47] Once HDs-loaded MBNCs were taken into the tumor cells by the endocytosis, GSH in the cells could cause the disassembly of HD-loaded MBNCs and release inner hydrophilic drugs, which had a chance to realize drug controlled release. The behavior might help to overcome

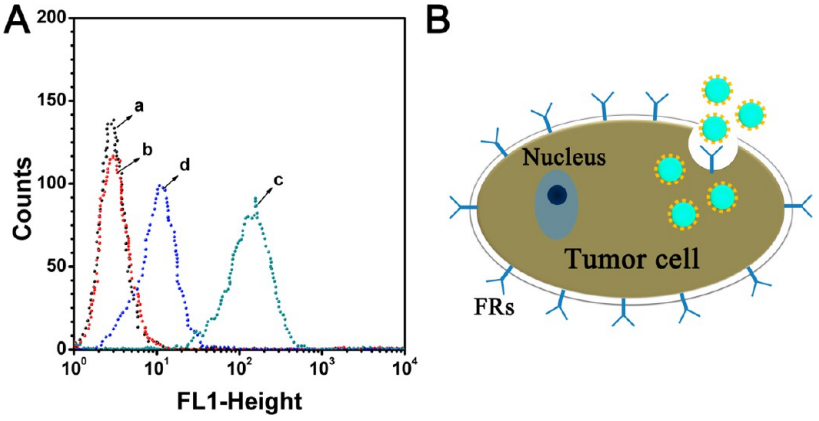

Figure 9. (A) Flow cytometry of HeLa cells incubated in different nutrient solutions: (a) pure serum-free medium, (b) pure serum-free medium after the pretreatment of FA, (c) serum-free medium with RhB-loaded MBNCs, and (d) serum-free medium with RhB-loaded MBNCs after the pretreatment of FA. (B) Schematic of cellular uptake of HD-loaded MBNCs.

DOI: 10.1021/acsami.5b05558
ACS Appl. Mater. Interfaces 2015, 7, 19390−19397

the multidrug resistance (MDR) of cancer cells.[48−50] Therefore, HD-loaded MBNCs had access to the physiological therapeutics as the drug carriers.

4. CONCLUSION

In summary, a facile approach based on the sonochemical technique was rationally designed to fabricate multifunctional BSA nanocapsules for hydrophilic drugs, and high-dose hydrophilic drugs were encapsulated successfully into the MBNCs. HD-loaded MBNCs had a satisfying size range and showed an excellent magnetic responsive ability. As the carriers, HD-loaded MBNCs showed attractive controlled release ability for HDs owing to their redox responsiveness and had access to the cellular uptake through the FA-dependent endocytosis. Accordingly, HDs-loaded MBNCs should be excellent candidates as smart carriers for the targeted delivery and controlled release of HDs. Furthermore, the facile sonochemical route provided a chance to solve the loading of hydrophilic drugs for the protein nanocapsules or microcapsules.

■ ASSOCIATED CONTENT

Supporting Information

The Supporting Information is available free of charge on the ACS Publications website at DOI: 10.1021/acsami.5b05558.

Results from analytical DSC; microphotograph; TG, DLS, FTIR, CLSM, UV−vis measurements; and camera images (PDF)

■ AUTHOR INFORMATION

Corresponding Author

*E-mail: cui_xj@jlu.edu.cn.

Notes

The authors declare no competing financial interest.

■ ACKNOWLEDGMENTS

This work was supported by the National Natural Science Foundation of China (Nos. 21104023 and 21106052) and the Key Program of the Science and Technology Department of Jilin Province, P. R. China (No. 20140204053GX). This work was also supported by the Graduate Innovation Fund of Jilin University (Project 2015039).

■ REFERENCES

(1) Poehlmann, M.; Grishenkov, D.; Kothapalli, S. V. V. N.; Härmark, J.; Hebert, H.; Philipp, A.; Hoeller, R.; Seuss, M.; Kuttner, C.; Margheritelli, S.; Paradossi, G.; Fery, A. On the Interplay of Shell Structure with Low- and High-Frequency Mechanics of Multifunctional Magnetic Microbubbles. *Soft Matter* **2014**, *10*, 214−226.

(2) An, Z.; Lu, G.; Möhwald, H.; Li, J. Self-Assembly of Human Serum Albumin (HSA) and l-α-Dimyristoylphosphatidic Acid (DMPA) Microcapsules for Controlled Drug Release. *Chem. - Eur. J.* **2004**, *10*, 5848−5852.

(3) Pretzl, M.; Neubauer, M.; Tekaat, M.; Kunert, C.; Kuttner, C.; Leon, G.; Berthier, D.; Erni, P.; Ouali, L.; Fery, A. Formation and Mechanical Characterization of Aminoplast Core/Shell Microcapsules. *ACS Appl. Mater. Interfaces* **2012**, *4*, 2940−2948.

(4) He, Q.; Cui, Y.; Li, J. Molecular Assembly and Application of Biomimetic Microcapsules. *Chem. Soc. Rev.* **2009**, *38*, 2292−2303.

(5) Lu, G.; An, Z.; Tao, C.; Li, J. Microcapsule Assembly of Human Serum Albumin at the Liquid/Liquid Interface by the Pendent Drop Technique. *Langmuir* **2004**, *20*, 8401−8403.

(6) Wu, Z.; Wu, Y.; He, W.; Lin, X.; Sun, J.; He, Q. Self-Propelled Polymer-Based Multilayer Nanorockets for Transportation and Drug Release. *Angew. Chem., Int. Ed.* **2013**, *52*, 7000−7003.

(7) Wu, Y.; Lin, X.; Wu, Z.; Möhwald, H.; He, Q. Self-Propelled Polymer Multilayer Janus Capsules for Effective Drug Delivery and Light-Triggered Release. *ACS Appl. Mater. Interfaces* **2014**, *6*, 10476−10481.

(8) Jeong, W. C.; Kim, S. H.; Yang, S. M. Photothermal Control of Membrane Permeability of Microcapsules for On-Demand Release. *ACS Appl. Mater. Interfaces* **2014**, *6*, 826−832.

(9) Suslick, K. S.; Grinstaff, M. W. Protein Microencapsulation of Nonaqueous Liquids. *J. Am. Chem. Soc.* **1990**, *112*, 7807−7809.

(10) Flannigan, D. J.; Suslick, K. S. Plasma Formation and Temperature Measurement during Single-Bubble Cavitation. *Nature* **2005**, *434*, 52−55.

(11) Wu, J.; Zhu, Y. J.; Cao, S. W.; Chen, F. Hierachically Nanostructured Mesoporous Spheres of Calcium Silicate Hydrate: Surfactant-Free Sonochemical Synthesis and Drug-Delivery System with Ultrahigh Drug-Loading Capacity. *Adv. Mater.* **2010**, *22*, 749−753.

(12) Gedanken, A. Preparation and Properties of Proteinaceous Microspheres Made Sonochemically. *Chem. - Eur. J.* **2008**, *14*, 3840−3853.

(13) Han, Y.; Shchukin, D.; Yang, J.; Simon, C. R.; Möhwald, H. Biocompatible Protein Nanocontainers for Controlled Drugs Release. *ACS Nano* **2010**, *4*, 2838−2844.

(14) Shimanovich, U.; Bernardes, G. J. L.; Knowles, T. P. J.; Cavaco-Paulo, A. Protein Micro- and Nano-Capsules for Biomedical Applications. *Chem. Soc. Rev.* **2014**, *43*, 1361−1371.

(15) Shimanovich, U.; Perelshtein, I.; Cavaco-Paulo, A.; Gedanken, A. Releasing Dye Encapsulated in Proteinaceous Microspheres on Conductive Fabrics by Electric Current. *ACS Appl. Mater. Interfaces* **2012**, *4*, 2926−2930.

(16) Cui, X.; Wang, B.; Zhong, S.; Li, Z.; Han, Y.; Wang, H.; Möhwald, H. Preparation of Protein Microcapsules with Narrow Size Distribution by Sonochemical Method. *Colloid Polym. Sci.* **2013**, *291*, 2271−2278.

(17) Santra, S.; Kaittanis, C.; Santiesteban, O. J.; Perez, J. M. Cell-Specific, Activatable, and Theranostic Prodrug for Dual-Targeted Cancer Imaging and Therapy. *J. Am. Chem. Soc.* **2011**, *133*, 16680−16688.

(18) Zhao, J.; Liu, J.; Xu, S.; Zhou, J.; Han, S.; Deng, L.; Zhang, J.; Liu, J.; Meng, A.; Dong, A. Graft Copolymer Nanoparticles with pH and Reduction Dual-Induced Disassemblable Property for Enhanced Intracellular Curcumin Release. *ACS Appl. Mater. Interfaces* **2013**, *5*, 13216−13226.

(19) Ojima, I. Guided Molecular Missiles for Tumor-Targeting Chemotherapy—Case Studies Using the Second-Generation Taxoids as Warheads. *Acc. Chem. Res.* **2008**, *41*, 108−119.

(20) Li, Z.; Zhang, C.; Wang, B.; Wang, H.; Chen, X.; Möhwald, H.; Cui, X. Sonochemical Fabrication of Dual-Targeted Redox-Responsive Smart Microcarriers. *ACS Appl. Mater. Interfaces* **2014**, *6*, 22166−22173.

(21) Li, Z.; Liu, S.; Wang, S.; Qiang, L.; Yang, T.; Wang, H.; Möhwald, H.; Cui, X. Synthesis of Folic Acid Functionalized Redox-Responsive Magnetic Proteinous Microcapsules for Targeted Drug Delivery. *J. Colloid Interface Sci.* **2015**, *450*, 325−331.

(22) Dong, H.; Mantha, V.; Matyjaszewski, K. Thermally Responsive $PM(EO)_2MA$ Magnetic Microgels via Activators Generated by Electron Transfer Atom Transfer Radical Polymerization in Miniemulsion. *Chem. Mater.* **2009**, *21*, 3965−3972.

(23) Lang, L.; Xu, Z. In Situ Synthesis of Porous Fe_3O_4/C Microbelts and Their Enhanced Electrochemical Performance for Lithium-Ion Batteries. *ACS Appl. Mater. Interfaces* **2013**, *5*, 1698−1703.

(24) Li, Z.; Qiang, L.; Zhong, S.; Wang, H.; Cui, X. Synthesis and Characterization of Monodisperse Magnetic Fe_3O_4@BSA Core-Shell Nanoparticles. *Colloids Surf., A* **2013**, *436*, 1145−1151.

(25) Cui, X.; Li, Z.; Zhong, S.; Wang, B.; Han, Y.; Wang, H.; Möhwald, H. A Facile Sonochemical Route for the Fabrication of Magnetic Protein Microcapsules for Targeted Delivery. *Chem. - Eur. J.* **2013**, *19*, 9485−9488.

DOI: 10.1021/acsami.5b05558
ACS Appl. Mater. Interfaces 2015, 7, 19390−19397

(26) Desai, N. P.; Soon-Shiong, P.; Sandford, P. A.; Grinstaff, M. W.; Suslick, K. S. Methods for *in Vivo* Delivery of Substantially Water Insoluble Pharmacologically Active Agents and Compositions Useful Therefor. U. S. Patent 5439686, 1995.
(27) Han, Y.; Radziuk, D.; Shchukin, D.; Möhwald, H. Sonochemical Synthesis of Magnetic Protein Container for Targeted Delivery. *Macromol. Rapid Commun.* **2008**, *29*, 1203−1207.
(28) Jeong, U.; Teng, X.; Wang, Y.; Yang, H.; Xia, Y. Superparamagnetic Colloids: Controlled Synthesis and Niche Applications. *Adv. Mater.* **2007**, *19*, 33−60.
(29) Mahmoudi, M.; Sant, S.; Wang, B.; Laurent, S.; Sen, T. Superparamagnetic Iron Oxide Nanoparticles (SPIONs): Development, Surface Modification and Applications in Chemotherapy. *Adv. Drug Delivery Rev.* **2011**, *63*, 24−26.
(30) Tziveleka, L. A.; Bilalis, P.; Chatzipavlidis, A.; Boukos, N.; Kordas, G. Development of Multiple Stimuli Responsive Magnetic Polymer Nanocontainers as Efficient Drug Delivery Systems. *Macromol. Biosci.* **2014**, *14*, 131−141.
(31) McBride, A. A.; Price, D. N.; Lamoureux, L. R.; Elmaoued, A. A.; Vargas, J. M.; Adolphi, N. L.; Muttil, P. Preparation and Characterization of Novel Magnetic Nano-in-Microparticles for Site-Specific Pulmonary Drug Delivery. *Mol. Pharmaceutics* **2013**, *10*, 3574−3581.
(32) Yang, X.; Grailer, J. J.; Pilla, S.; Steeber, D. A.; Gong, S. Tumor-Targeting, pH-Responsive, and Stable Unimolecular Micelles as Drug Nanocarriers for Targeted Cancer Therapy. *Bioconjugate Chem.* **2010**, *21*, 496−504.
(33) Yoo, M. K.; Park, I. K.; Lim, H. T.; Lee, S. J.; Jiang, H. L.; Kim, Y. K.; Choi, Y. J.; Cho, M. H.; Cho, C. S. Folate-PEG-Superparamagnetic Iron Oxide Nanoparticles for Lung Cancer Imaging. *Acta Biomater.* **2012**, *8*, 3005−3013.
(34) Li, K.; Xiang, Y.; Wang, X.; Li, J.; Hu, R.; Tong, A.; Tang, B. Z. Reversible Photochromic System Based on Rhodamine B Salicylaldehyde Hydrazone Metal Complex. *J. Am. Chem. Soc.* **2014**, *136*, 1643−1649.
(35) Soylak, M.; Unsal, Y. E.; Yilmaz, E.; Tuzen, M. Determination of Rhodamine B in Soft Drink, Waste Water and Lipstick Samples after Solid Phase Extraction. *Food Chem. Toxicol.* **2011**, *49*, 1796−1799.
(36) Quesada, M.; Muniesa, C.; Botella, P. Hybrid PLGA-Organosilica Nanoparticles with Redox-Sensitive Molecular Gates. *Chem. Mater.* **2013**, *25*, 2597−2602.
(37) Lee, M. H.; Yang, Z.; Lim, C. W.; Lee, Y. H.; Dongbang, S.; Kang, C.; Kim, J. S. Disulfide-Cleavage-Triggered Chemosensors and Their Biological Applications. *Chem. Rev.* **2013**, *113*, 5071−5109.
(38) Lee, M. H.; Kim, J. Y.; Han, J. H.; Bhuniya, S.; Sessler, J. L.; Kang, C.; Kim, J. S. Direct Fluorescence Monitoring of the Delivery and Cellular Uptake of a Cancer-Targeted RGD Peptide-Appended Naphthalimide Theragnostic Prodrug. *J. Am. Chem. Soc.* **2012**, *134*, 12668−12674.
(39) Gao, L.; Fei, J.; Zhao, J.; Cui, W.; Cui, Y.; Li, J. pH- and Redox-Responsive Polysaccharide-Based Microcapsules with Autofluorescence for Biomedical Applications. *Chem. - Eur. J.* **2012**, *18*, 3185−3192.
(40) Fu, H.; Pan, C.; Yao, W.; Zhu, Y. Visible-Light-Induced Degradation of Rhodamine B by Nanosized Bi_2WO_6. *J. Phys. Chem. B* **2005**, *109*, 22432−22439.
(41) Wang, G.; Xu, X.; Qiu, L.; Dong, Y.; Li, Z.; Zhang, C. Dual Responsive Enzyme Mimicking Activity of AgX (X = Cl, Br, I) Nanoparticles and Its Application for Cancer Cell Detection. *ACS Appl. Mater. Interfaces* **2014**, *6*, 6434−6442.
(42) Lu, H.; Chang, Y.; Fan, N.; Wang, L.; Lai, N.; Yang, C.; Wu, L.; Ho, J. A. Synergism Through Combination of Chemotherapy and Oxidative Stress-Induced Autophagy in A549 Lung Cancer Cells Using Redox-Responsive Nanohybrids: A New Strategy for Cancer Therapy. *Biomaterials* **2015**, *42*, 30−41.
(43) Hu, S. H.; Chen, Y. W.; Hung, W. T.; Chen, I. W.; Chen, S. Y. Quantum-Dot-Tagged Reduced Graphene Oxide Nanocomposites for Bright Fluorescence Bioimaging and Photothermal Therapy Monitored In Situ. *Adv. Mater.* **2012**, *24*, 1748−1754.
(44) Hu, C.; Liu, Y.; Qin, J.; Nie, G.; Lei, B.; Xiao, Y.; Zheng, M.; Rong, J. Fabrication of Reduced Graphene Oxide and Sliver Nanoparticle Hybrids for Raman Detection of Absorbed Folic Acid: A Potential Cancer Diagnostic Probe. *ACS Appl. Mater. Interfaces* **2013**, *5*, 4760−4768.
(45) Wen, H. Y.; Dong, H. Q.; Xie, W. J.; Li, Y. Y.; Wang, K.; Pauletti, G. M.; Shi, D. L. Rapidly Disassembling Nanomicelles with Disulfide-Linked PEG Shells for Glutathione-Mediated Intracellular Drug Delivery. *Chem. Commun.* **2011**, *47*, 3550−3552.
(46) Sharma, S. Metal Dependent Catalytic Hydrogenation of Nitroarenes over Water-Soluble Glutathione Capped Metal Nanoparticles. *J. Colloid Interface Sci.* **2015**, *441*, 25−29.
(47) Zhang, Y.; Wang, M.; Zheng, Y.; Tan, H.; Hsu, B. Y.; Yang, Z.; Wong, S. Y.; Chang, A. Y.; Choolani, M.; Li, X.; Wang, J. PEOlated Micelle/Silica as Dual-Layer Protection of Quantum Dots for Stable and Targeted Bioimaging. *Chem. Mater.* **2013**, *25*, 2976−2985.
(48) Vivek, R.; Thangam, R.; NipunBabu, V.; Rejeeth, C.; Sivasubramanian, S.; Gunasekaran, P.; Muthuchelian, K.; Kannan, S. Multifunctional HER2-Antibody Conjugated Polymeric Nanocarrier-Based Drug Delivery System for Multi-Drug-Resistant Breast Cancer Therapy. *ACS Appl. Mater. Interfaces* **2014**, *6*, 6469−6480.
(49) Kelley, E. G.; Albert, J. N. L.; Sullivan, M. O.; Epps, T. H., III Stimuli-Responsive Copolymer Solution and Surface Assemblies for Biomedical Applications. *Chem. Soc. Rev.* **2013**, *42*, 7057−7071.
(50) Chen, S.; Ruan, Y.; Brown, J. D.; Gallucci, J.; Maslak, V.; Hadad, C. M.; Badjic, J. D. Assembly of Amphiphilic Baskets into Stimuli-Responsive Vesicles. Developing a Strategy for the Detection of Organophosphorus Chemical Nerve Agents. *J. Am. Chem. Soc.* **2013**, *135*, 14964−14967.

DOI: 10.1021/acsami.5b05558
ACS Appl. Mater. Interfaces 2015, 7, 19390−19397